

Near-field Optical Magnetometry and Magnetic Imaging of Nanomagnets

Naser Qureshi^{*a)}, Aaron R. Hawkins^{b)}, Holger Schmidt^{a)}

^{a)}School of Engineering, University of California, 1156 High Street, Santa Cruz, CA 95064

^{b)}Department of Electrical and Computer Engineering, Brigham Young University, Provo UT 84602

ABSTRACT

We present an all-optical approach to detecting magnetization reversal events in submicron ferromagnetic structures that is non-perturbative and compatible with ultrafast optical techniques. We demonstrate experimentally that structures much smaller than the wavelength of light can be probed using both near-field and far-field laser techniques combined with a cavity Kerr enhancement technique and two different polarimetry methods. Controlled magnetization reversal events are detected in nickel magnets approaching the 100nm scale. This leads to a promising way to measure sub-picosecond dynamics of nanomagnets for fast device applications.

Keywords: near-field polarimetry, near-field scanning optical microscopy, nanomagnetism, MOKE.

*naser@soe.ucsc.edu

1. INTRODUCTION

Optical methods based on the magneto-optic Kerr effect (MOKE) are used in the study of magnetization dynamics in ferromagnetic materials and provide a spatially resolved non-invasive approach that allows for higher temporal resolution than other commonly used methods¹. There has been great interest recently in the magnetization reversal dynamics of single domain nanomagnets from both a scientific perspective and for applications in high speed devices and high density information storage^{2,3}, which has fueled interest in the use of MOKE-based magnetometry. The typical size of a single domain magnet, however, is 100nm or less and the spatial resolution of MOKE measurements has been limited by the ability of conventional microscope objectives to focus laser light. When the magnet under study is much smaller than the laser spot size, the Kerr signal is sharply reduced and the signal to noise ratio in typical MOKE measurements makes it impossible to detect magnetization reversal events. Optical magnetization measurements on an individual single domain nanomagnet have therefore been elusive, and studies have thus far involved arrays of devices where signals are multiplied by the number of devices⁴. This work is motivated by the need to improve the spatial resolution of optical magnetization measurements and magnetic imaging in order to enable the time-resolved study of single nanomagnets with sub-picosecond resolution. We here present results in the development of a near-field MOKE imaging instrument designed to be compatible with existing ultrafast techniques with sufficient spatial resolution to probe an isolated single domain magnet.

We have developed a reflection mode near-field optical imaging system with submicron resolution and have used it to perform linear polarization rotation measurements to detect magnetization reversal events in individual magnetic structures with a range of sizes approaching 100nm, previously inaccessible to conventional MOKE microscopy. Typical polarization rotations are smaller than 0.1° and their measurement through a mechanically scanned near-field aperture represents a significant challenge. Although near-field MOKE measurements have been demonstrated⁵, measurements on 100nm structures have not yet been published. In this work we discuss new developments in the use of a cavity Kerr enhancement technique combined with lock-in methods to improve the polarization sensitivity of these measurements. Here, signal to noise ratio is improved by resonantly enhancing the

MOKE signal with the use of a Fabry-Perot cavity applied in the form of a dielectric coating (Fig. 1a). We present the results of two different lock-in methods developed for polarimetry under these conditions and describe how the effective microradian sensitivity can be used to probe nanomagnets.

We begin in Section 2 with a review of some recent developments in the use of MOKE and cavity Kerr enhancement in magnetometry. In Section 3 we describe in detail experimental approaches to probing magneto-optic rotations combined with both near-field and far-field microscopy.

2. MAGNETO-OPTIC KERR EFFECT AND ITS ENHANCEMENT

In the polar magneto-optic Kerr effect, linearly polarized light impinging normal to the surface of a reflective magnetized material experiences a rotation in the plane of polarization upon reflection⁶. This results from the fact that the material has different refractive indices for the two circularly polarized components of the light. This effect is used extensively in research and in industry as a non-invasive probe of magnetization in reflective thin films. Light is often focused using a microscope objective in order to obtain spatial resolution and some groups have combined this with ultrafast pulsed laser techniques to study the spatial evolution of magnetization¹.

It has been known for more than half a century that the use of a thin dielectric film to form a Fabry-Perot cavity on the magnetic surface leads to multiple reflections and therefore multiple Kerr rotations which can lead to a resonantly enhanced polarization rotation emerging from the cavity^{6,7}. Enhancement of the Kerr rotation by factors of up to 4 have been observed by several groups and more recently a factor of 16 was seen using a bi-layer film⁸.

Theoretically, for a single dielectric layer it is straightforward to calculate the polarization rotation from the cavity by summing the partial waves for each reflection in the cavity as is done in textbooks. With an appropriate choice of lossless dielectric constant, arbitrarily large enhancements are in principle possible⁸ and for a dielectric film on nickel, this is shown in Fig. 1b. This optimal case calls for a lossless coating with dielectric constant $n_2 \approx 3.9$ on a nickel surface, which is not readily available at visible wavelengths. Common dielectrics such as silicon dioxide and silicon nitride applied to a magnetized nickel surface yield Kerr enhancement factors of 2.5 and 5 respectively.

More general methods for calculating the enhancement exist for any sequence of magnetic films⁹, and for the case of a single magnetic layer with one or more possibly lossy dielectric coatings, a simple scattering matrix approach has been introduced by the authors⁸. Here, a linearly polarized beam of vacuum wavelength λ is incident on the top layer and an incident polarization E_i in the x-direction is assumed. Reflection coefficients \mathbf{r}_n are derived from the material refractive indices and described as 2x2 matrices with complex coefficients, such that the x- and y- linearly polarized components form the basis vectors. In this way, the reflection coefficient takes into account polarization mixing. For each dielectric layer in the coating, a T-matrix is constructed. For a single layer dielectric coating, the T-matrix is simply that for a Fabry-Perot cavity with reflection coefficients replaced by matrices, so that

$$\mathbf{T}^{(1)} = (\mathbf{t}_1 \mathbf{t}_2)^{-1} \begin{bmatrix} \mathbf{I} e^{i\theta} + \mathbf{r}_1 \mathbf{r}_2 e^{-i\theta} & \mathbf{r}_2 e^{i\theta} + \mathbf{r}_1 e^{-i\theta} \\ \mathbf{r}_1 e^{i\theta} + \mathbf{r}_2 e^{-i\theta} & \mathbf{I} e^{-i\theta} + \mathbf{r}_1 \mathbf{r}_2 e^{i\theta} \end{bmatrix} \quad (2.1)$$

where \mathbf{I} is the 2x2 identity matrix and $\theta = 2\pi n_2 L_2 / \lambda$ is the phase shift within the dielectric of thickness L_1 , and \mathbf{t}_1 and \mathbf{t}_2 are transmission matrices. The scattering matrix \mathbf{S} has components that are themselves 2x2 matrices, and the only one required to evaluate reflections from the system is

$$\mathbf{S}_{11} = (\mathbf{T}_{21})^{-1} \mathbf{T}_{11}. \quad (2.2)$$

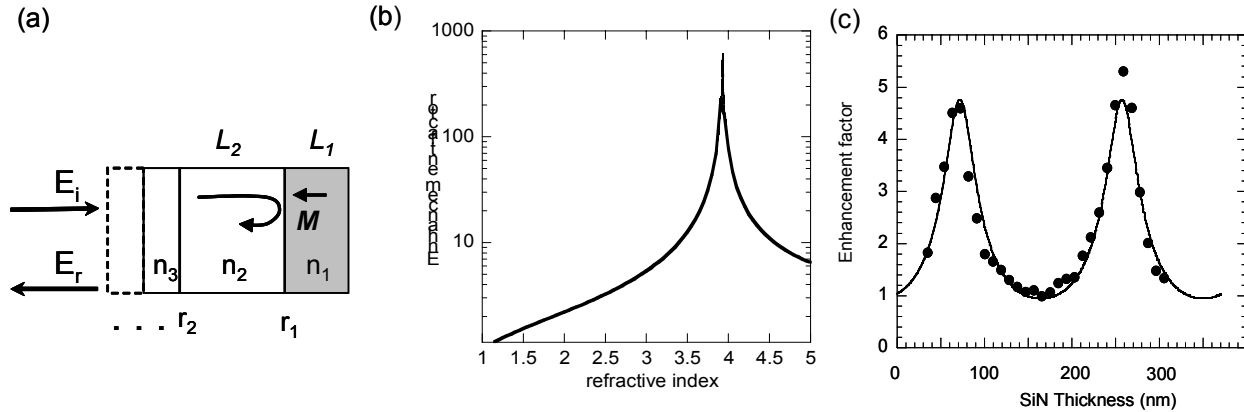


Fig. 1. (a) One or more dielectric layers on a magnetic material lead to multiple reflections. (b) Enhancement factor for a lossless dielectric as a function of dielectric refractive index, and enhancement as a function of thickness for a single layer of SiN on nickel; theory (lines) and experiment (dots).

The reflected electric field is then

$$\mathbf{E}_r = \mathbf{S}_{11} \mathbf{E}_i \quad (2.3)$$

and the total polarization rotation from the cavity is

$$\Phi = \arctan \left[\frac{(E_r)_y}{(E_r)_x} \right]. \quad (2.4)$$

This procedure is readily extended to k dielectric layers by repeatedly multiplying (2.1) by additional T-matrices, details of which are given in Ref. 8, and lends itself easily to numerical simulation.

A general result for such coatings is that the Kerr enhancement occurs for specific dielectric thicknesses that correspond to cavity resonance and depend on the complex refractive indices of the ferromagnetic and dielectric materials used. This theoretical treatment predicts that with a single dielectric coating in which the reflectivity of the dielectric-air interface matches that of the ferromagnet-dielectric interface, the enhancement becomes essentially infinite. A similar situation can also be realized with multilayers. For example, one can find combinations of silicon dioxide and gold layers for which the theoretical treatment predicts essentially infinite enhancements even if there is loss in the metal layer. In practice, however, as we tune the cavity to increase the enhancement, there is a commensurate decrease in the intensity of light reflected from the cavity so that this ideal case would be impossible to measure. The largest observed enhancement published so far is 16 using a gold-SiO₂ coating⁸ and is limited by the surface roughness of the metal and the consequent broadening of the cavity resonance.

There is therefore a trade-off involved in the use of this cavity method to improve signal to noise ratio in polarimetry: a larger enhancement leads to larger polarization rotation signal but at the same time leads to a decrease in the intensity of light that experiences this rotation. It is not clear from this theory whether or not there is any advantage to applying it to magnetic structures and we approach the question experimentally in the next section. Furthermore, if a dielectric coating is applied to a submicron magnetic structure, a three-dimensional cavity structure is created unlike the one-dimensional problem treated in the above theory. In the next section, we demonstrate experimentally the applicability and advantages of cavity Kerr enhancement with such small structures.

3. SPATIALLY RESOLVED POLARIMETRY

3.1 Samples and microscopy

The magnetic structures considered here are nickel squares ranging from 10 μm to 250nm in length. These were prepared using electron beam lithography on a silicon substrate followed by deposition of 150nm of nickel using electron beam deposition and lift-off. The structures were then coated with 70nm of silicon nitride using a plasma-enhanced chemical vapor deposition system. This thickness provides an optimal enhancement for this material combination for light at 780nm, which has been verified both theoretically and experimentally in continuous thin films⁸. The minimum distance between nickel squares was 5 μm , which ensured that a laser beam could be focused onto only one square at a time. An additional sample with a continuous film of nickel was also used to verify that in an applied field of approximately 0.1T, the nickel can be magnetized to saturation and a complete magnetization reversal results in a change in Kerr rotation of approximately 1 $^\circ$ from the material.

Magneto-optic Kerr measurements were performed using focused linearly polarized light from a 780nm laser diode with 25mW output power, modulated at 1kHz. We consider two different approaches to achieving the necessary spatial resolution: (i) In a far-field approach, the light is focused to a spot size of approximately 2 μm onto the structure of interest using a 40X microscope objective, and the sample is mounted on a fine x-y-z stage in order to align the beam with the structure and optimize the focus. A small part of the reflected beam is sampled and focused on a CCD camera with an additional lens in order to form an image on the sample to facilitate alignment. The rest of the beam is detected through a polarization analyzer. This is depicted in Fig. 2a; (ii) In a near-field approach, light is focused onto the sample using a standard achromatic lens at close to normal incidence and the reflected light is collected using a scanned tapered optical fiber with a submicron aperture. The light emerging from the fiber is then collimated and sent to a polarization analyzer. This is shown schematically in Fig 2b.

In both approaches, a permanent NdB magnet with surface field of approximately 0.1T is placed behind the sample to magnetize the nickel structure. The permanent magnet is then rotated to reverse the applied field and the change in polarization is detected. In the next section, we discuss results with three different polarimetry schemes.

3.2 Polarimetry

The simplest polarization analyzer is formed by placing a polarizer at 45 $^\circ$ to the incident light after the sample and collecting light with a silicon photodiode and a lock-in amplifier at the laser modulation frequency (Fig. 3a). Small polarization changes result in small intensity changes in the detector. Although this scheme has the advantage that 50% of light reflected from the sample reaches the detector, its accuracy is limited by the stability of the laser beam and we find a noise floor of 0.01 $^\circ$ in a typical near-field measurement and was sufficient to detect magnetization reversal events in a continuous nickel film as well as an SiN-coated one. In the case of a near-field measurement, however, this scheme had a typical noise level of 0.5 $^\circ$ and was insufficient to detect any magnetization reversal.

In a more refined approach, a permanent magnet rotating at 25Hz with a surface field of approximately 0.1T was placed behind the sample in order to periodically reverse the magnetization of the nickel structures (Fig. 3b). A polarizer placed before the detector was set at 45 $^\circ$ to the input beam so that the polarization rotation resulting from the magnetic field was detectable as a modulation in the intensity at the photodiode. This modulation I_{mag} was detected using a lock-in amplifier at the magnet rotation frequency ω_{mag} . The average intensity I_{laser} of the reflected beam was measured with another lock-in amplifier set at the laser modulation frequency. A small Kerr rotation ϕ is then determined as

$$\phi \approx \frac{I_{mag}}{2I_{laser}} \quad (3.1)$$

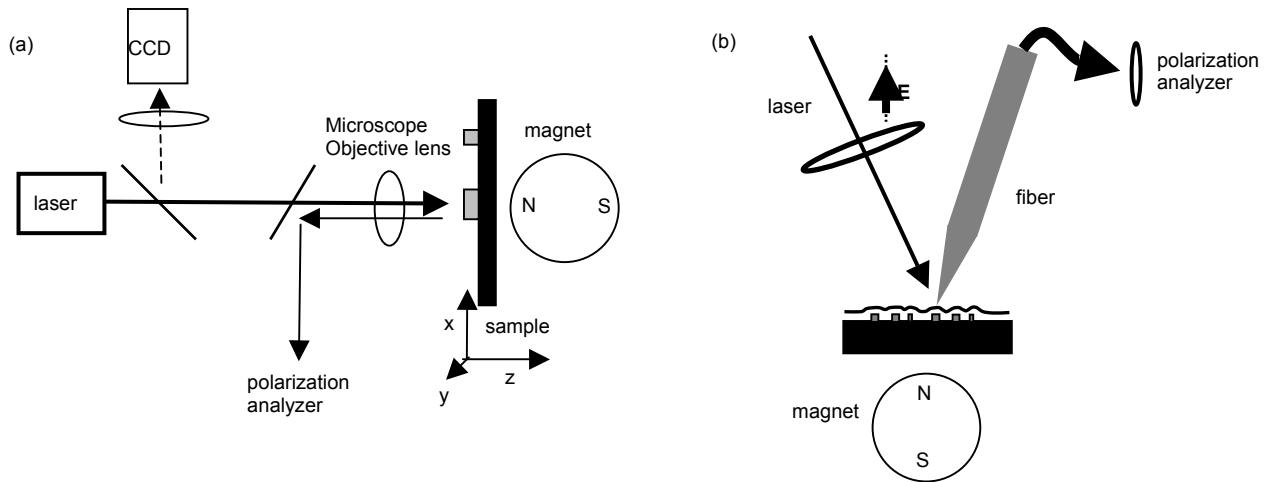


Fig. 2. (a) A far-field MOKE apparatus using a microscope objective lens. (b) A near-field MOKE apparatus using a near-field scanning optical microscope.

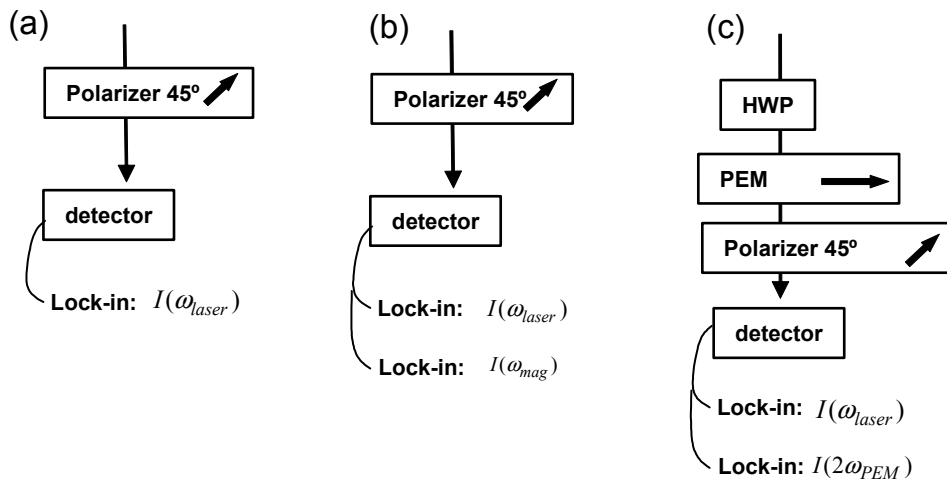


Fig. 3. Three polarimetry schemes used in this work: (a) changes in intensity are used to deduce polarization changes, (b) a signal proportional to an applied a.c. magnetic field modulation frequency yields the Kerr rotation and (c) a signal proportional to the twice the photoelastic modulation frequency gives the Kerr rotation.

in radians. We limit ourselves to an analysis that assumes purely linear polarization, because no significant ellipticity was observed.

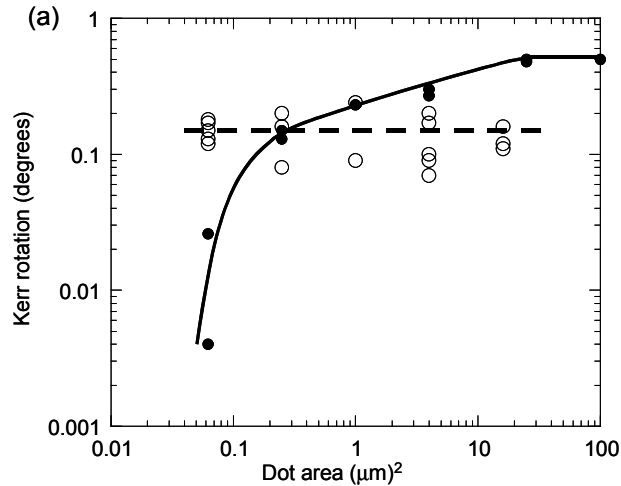


Fig. 4. Maximum Kerr rotation from nickel square structures of various sizes coated with 70nm of SiN, measured through the same near-field aperture optical fiber (o) and through a far-field microscope objective lens (●)¹⁰.

In a far-field measurement, it was possible to discriminate a polarization signal of $I_{mag} = 6 \times 10^{-5} I_{laser}$ which led to a noise floor of 0.002° ($34 \mu\text{rad}$).

In order to analyze the resolution limit of this far-field approach, magnetic structures were scanned relative to the beam and spatially resolved Kerr rotation measurements were obtained for both SiN-coated and uncoated structures. Structures larger than the laser spot size gave the same Kerr signal as measured from a continuous film: 0.1° for uncoated nickel and 0.5° for coated nickel. As expected, the measured Kerr rotation decreased sharply for nickel structures smaller than the spot size (Fig. 4). The smallest uncoated structure for which we could resolve a Kerr signal was a $1 \mu\text{m}$ square, which makes it impossible to resolve the magnetization of an uncoated single domain magnet with this measurement scheme.

The addition of a cavity enhancement layer improved the far-field resolution. With the SiN-coated samples, we were able to resolve the Kerr rotation from a $0.25 \mu\text{m}$ square with the same noise floor, a factor of 16 smaller in area, even though the Kerr rotation was enhanced by a factor of only 5. This is consistent with the fact that the SiN layer not only increases the Kerr rotation, but also provides a greater reflectivity contrast between the nickel and surrounding silicon so that a smaller proportion of the signal at the detector is reflected from the silicon. From this we can conclude that the cavity Kerr enhancement continues to work when the structure under study is smaller than the wavelength of light in all dimensions.

To test the resolution of this polarimetry scheme in the near field, a near-field scanning optical microscopy system (NSOM) was developed to carry tapered single mode optical fibers and to function in the presence of large magnetic fields. Fibers were prepared using a meniscus etching method¹¹ with a taper angle chosen for high throughput and polarization maintaining properties, and coated with 150nm of aluminum in an electron beam evaporator to produce an aperture of less than 500nm. The NSOM was operated in collection mode: 40mW of light from a 780nm laser diode was focused onto the samples using a diffraction-limited lens at an angle close to vertical. The reflected light collected from the scanning fiber tip was typically on the order of $1 \mu\text{W}$ in intensity, and was then detected through a polarization analyzer as described above. Details of the measurement system are provided in Ref. 10.

The noise floor in these measurements was 0.05° , a factor of 10 better than in the polarimetry scheme described earlier. We failed to observe the expected 0.05 - 0.1° Kerr signals from any of the uncoated nickel structures or from a continuous nickel film of the same thickness. Combined with the use of a 70nm SiN Kerr enhancement coating, however, this scheme was sufficient to observe clear Kerr rotation signals whose magnitude varied between 0.1° and 0.5°

depending on the exact position of the tip relative to the sample (Fig. 4). The Kerr rotation signal does not decrease systematically as the structure being measured gets smaller. For the smallest structures (0.25 μm in length), we find signals typically an order of magnitude larger than measured with conventional far-field microscopy. We thus find that magnetization reversal can be detected using cavity Kerr enhancement with near-field resolution in structures much smaller than the wavelength of light.

The primary disadvantage of the above detection scheme is that the polarization signal arises from multiple polarization rotations in the structure of interest averaged over several seconds. In the context of real devices, it would be desirable to detect single magnetization reversal events in nanomagnets. To this end, we consider the scheme depicted in Fig. 3c. The polarization of light reflected from the sample is adjusted using a half wave plate such that it is 90° to the axis of a photoelastic modulator (PEM). The retardance of light polarized along the PEM axis is modulated at a frequency of 50kHz and an amplitude of 180°. The PEM is followed by a polarizer set at 45°. Small rotations in linear polarization entering the analyzer result in a signal at twice the PEM frequency¹² which is detected with a lock-in amplifier. A stationary permanent magnet is placed underneath the sample and then reversed a few seconds later to reverse the sample magnetization. The resulting change in polarization ϕ is then deduced from a change in the ratio of the PEM signal and the total reflected intensity: $\phi = I(2\omega_{PEM})/[4J_2(\pi)I(\omega_{laser})]$ ¹².

In a far-field measurement with this PEM scheme, we found a noise floor of less than 0.0005°, better than that observed in the other two schemes. We were able to detect individual magnetization reversal events in uncoated structures as small as 0.5 μm . In the case of SiN-coated structures, magnetization reversal events in 250nm structures were also detected and the signal to noise ratio was better than that in the rotating magnet scheme. In the near-field measurement on SiN-coated structures, we detected single magnetization reversal events in 250nm magnets with typical signal to noise ratios in the range of 5-10.

4. CONCLUSIONS

In conclusion, we have demonstrated both near-field and far-field all-optical laser probes of magnetization reversal in individual magnets as small as 250nm. We have seen that a polarimetry scheme based on photoelastic modulation combined with a near-field scanning optical microscope and the use of cavity Kerr enhancement provides the necessary spatial resolution and polarization sensitivity to probe single magnetization reversal events in individual 250nm magnets. In addition, we find that the sensitivity of this near-field measurement does not decline as the magnet size is reduced. We therefore expect this approach to allow magnetization reversal measurements on magnets on the scale of 100nm and smaller. The all-optical nature of this method makes it compatible with pulsed optical techniques and can be extended to measurements of magnetization dynamics in magnetic structures.

5. ACKNOWLEDGMENTS

The authors would like to thank Andrew Cleland and J. Sequoyah Aldridge of U.C. Santa Barbara for their help with the electron beam lithography aspects of this work.

REFERENCES

1. M. R. Freeman, W. K. Heibert and A. Stankiewicz, *J. Appl. Phys.* **83**, 6217 (1998).
2. S.K. Nair and R.M.H.New, *IEEE Trans. On Magn.*, **34**, 1916, (1998).
3. C. A. Ross, M. Hwang, M. Shima, J. Y. Cheng, M. Farhoud, T. A. Savas, H. I. Smith, W. Schwarzacher, F. M Ross, M. Redjdal, F. B. Humphrey, *Phys. Rev. B* **65**, 144417 (2002).
4. W. C. Uhlig, H. Li, B. S. Han, J. Shi, *J. Appl. Phys.* **91**, 6943 (2002).
5. P. Fumagalli, *et al.*, *Appl. Phys. Lett* **22**, 2803 (1998).
6. A. V. Sokolov, "Optical Properties of Metals", p. 311, Blackie & Sons, London 1967.
7. Nakamura K, Asaka T, Asari S, Ota Y, Itoh A., *IEEE Transactions on Magnetism*, **21**, 165 (1985).
8. N. Qureshi, H. Schmidt, A. R. Hawkins, *Appl. Phys. Lett.* **85**, 431 (2004).
9. M. Mansuripur, *J. Appl. Phys.* **67**, 6466 (1990).
10. N. Qureshi, H. Schmidt, A. R. Hawkins, *SPIE Vol.* 5515, (2004).
11. S. Monobe, M. Ohtsu, *Journal of Lightwave Tech.*, **14**, 2231 (1996).
12. J. Cerne, D. C. Schmadel, L. B. Rigal, H. D. Drew, *Rev. Sci. Instr.* **74**, 4755 (2003).